Nonlinear Processes in Geophysics (1996) 3: 13 - 22

Nonlinear Processes in Geophysics

Scaling properties of palaeomagnetic reversal sequence

S. S. Ivanov

Department of Geophysics, P.P. Shirshov Institute of Oceanology, Russian Academy of Sciences, 23, Krasikova St., 117218 Moscow, Russia

Received 1 February 1995 - Accepted 28 August 1995 - Communicated by D. Schertzer

Abstract. The history of reversals of main geomagnetic field during last 160 My is analyzed as a sequence of events, presented as a point set on the time axis. Different techniques were applied including the method of box-counting, dispersion counter-scaling, multifractal analysis and examination of attractor behavior in multidimensional phase space. The existence of a crossover point at time interval 0.5-1.0 My was clearly identified, dividing the whole time range into two subranges with different scaling properties. The long-term subrange is characterized by monofractal dimension 0.88 and by an attractor, whose correlation dimension converges to 1.0, that provides evidence of a deterministic dynamical system in this subrange, similar to most existing dynamo models. In the short-term subrange the fractal dimension estimated by different methods varies from 0.47 to 0.88 and the dimensionality of the attractor is obtained to be about 3.7. These results are discussed in terms of non-linear superposition of processes in the Earth's geospheres.

1 Introduction

In recent years estimation of self-similar properties (scaling) of manifestations of various geophysical processes has become more and more promising from the point of view of theoretical aspects of their driving mechanisms. During the last decade statistical scale invariance was found to be an intrinsic quality of numerous geographical, geological and geophysical features (Mandelbrot, 1983; Turcotte, 1989; Korvin, 1992, and others).

In this context one of the more interesting phenomena is the geomagnetic reversal sequence that reflects the history of changes of polarity of the main geomagnetic field (GMF). Ever since the origin of the reversal pattern during the last 100 My became sufficiently clear, various attempts have been made to interpret the sequence as a result of a stochastic process (i.e. Nadai, 1970), or as a superposition of aperiodic and periodic constituents (Mazaud et. al., 1983).

At the same time the idea of essential non-linearity of the processes in the liquid Earth's core responsible for the main GMF was elaborated, followed by a series of numerical simulation models (Rikitake, 1958; Lorenz, 1963; Robbins, 1976; Chillingworth and Holmes, 1980). In this context it was reasonable to suppose that the sequence as a whole may present a fractal set with scale-invariant properties characteristic of various non-linear dynamic systems (Barenblatt, 1978, Sagdeyev et. al., 1988). The sequence of GMF reversals provides a well-documented record of the behaviour of such a system during more than 150 My and gives an excellent opportunity to test the hypothesis of self-similarity.

2 Data

As a base for calculations we have taken the generally accepted geomagnetic polarity time scale compiled by A.Cox (1982) that covers the last 160 My (Fig. 1). Though some new detailed versions of paleomagnetic scale have been suggested (Hilgen, 1991a, b; Shackleton et al., 1990) they deal only with the most recent events (down to the Miocene/Pliocene boundary, that is about 5.3 Ma), and we found it reasonable not to revise Cox's scale in order to keep relative uniformity of accuracy of data. Reversal times in more recent scales differ from those of the Cox's scale by only a few per cent, and this scale is referred to as a sufficiently reliable base for statistical analysis (Lowrie, 1991).

Ages (dates) of geomagnetic inversion that indicate the borders of intervals with different GMF polarity are presented in this scale with an accuracy of 0.01 My. This is close to the theoretical limit since the very process of polarity change may last approximately 3.5-5.0 Ky (Prevot et al., 1985). The authors of this scale claim that it contains all of the chrons longer than 0.1 My, but some subchrons of lesser duration may be omitted. In this study

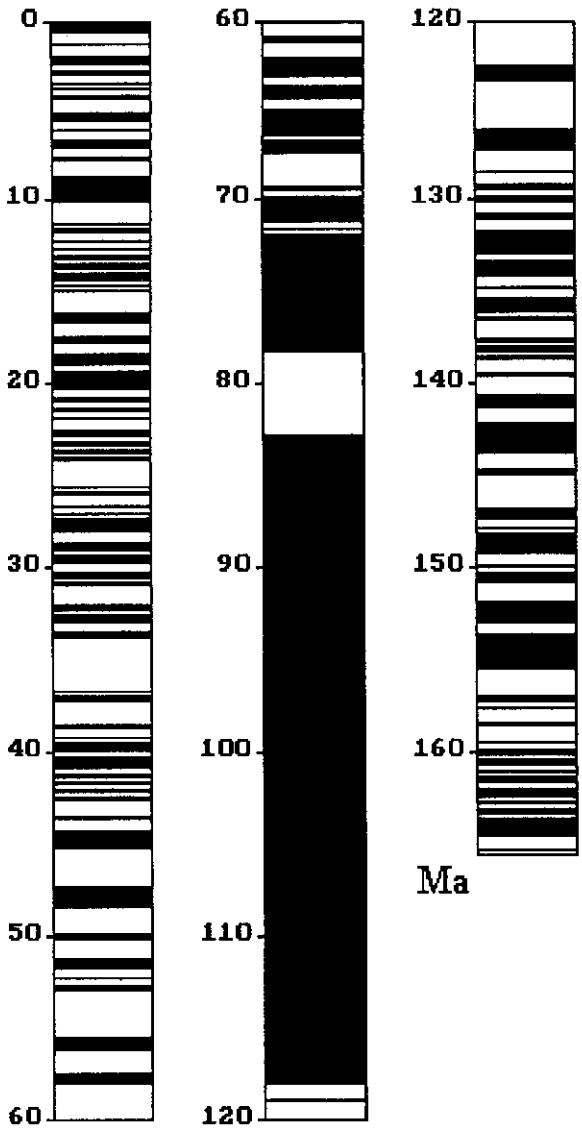

Fig. 1. Palaeomagnetic scale - history of reversals of main dipole geomagnetic field during last 160 My. Black stripes represent epochs of direct magnetic polarity (after Cox,1982).

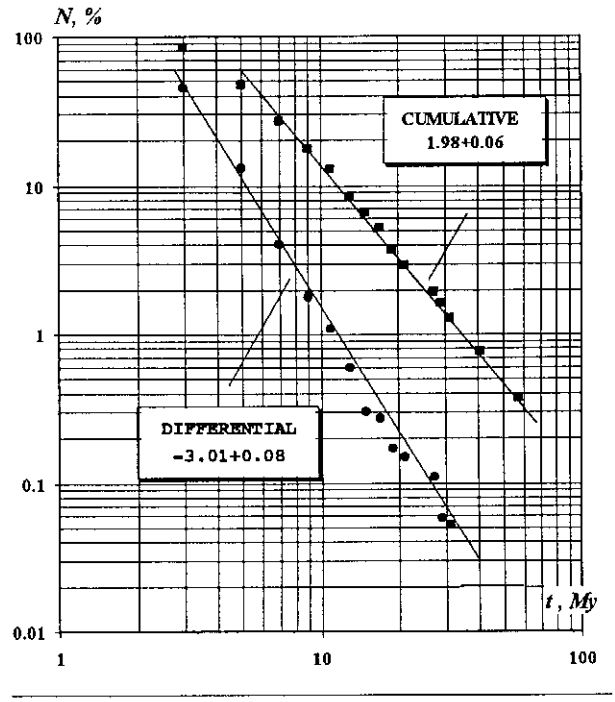

Fig. 2. Cumulative (squares) and differential (circles) distribution functions of intervals of constant polarity with respect to their length. Straight lines show the best least-square fit of power law approximation.

we accept that average conventional scale resolution is about 0.1 My though the accuracy of determination of individual events may be one order higher. It must be taken into account that the scale contains some episodes with duration of 0.01 My, so its effective accuracy lies within the interval 0.01-0.1 My, and accepted value of scale resolution is a rather rough estimate. The fact that each event on the time axis is defined with the declared accuracy of 0.01 My gives a formal base for analysis of scaling behavior down to this limit. For example, the box-counting procedure is valid here, because each event cannot occupy more than one box of 0.01 My width, and a box of 0.02 My may contain (and sometimes really contains) two adjacent but different events. Nevertheless one must bear in mind that the results obtained for the time span from 0.01 to 0.1 My are less reliable than those for greater intervals.

3 Results

3.1 Distribution of intervals

About 300 reversals are recorded during the period of 160 My so the average length (duration) of an interval with constant polarity is approximately 0.5 My. Let us examine the distribution of intervals with respect to their length for the entire scale.

The most representative statistical characteristic of the distribution is the integral distribution curve $N(t)$ (Fig.2) showing the relative quantity of intervals longer than t with the step length of 0.2 My. It is evident from the figure that for time intervals greater than 0.8-1.0 My the integral curve on a double logarithmic scale may be perfectly approximated with a straight line

$$\log N = \log 11.5 - (2.01 \pm 0.07) \cdot \log t$$

or

$$N = 11.5 \cdot t^{-2}, \qquad (1)$$

which proves the power-law character of the distribution and may indicate its fractality.

Figure 2 presents also the differential distribution curve, i.e. density of lengths distribution with the same time step. In order to satisfy the normalizing conditions the numbers dN within the time interval $[\ t\text{-}\Delta t..t\text{+}\Delta t\ ]$ are recalculated with respect to the position of the interval on the t axis according to

$$\Delta N(t) \rightarrow \frac{\Delta N(t)}{\log(t+\Delta t) - \log(t-\Delta t)}$$

for $\Delta t = 0.1$ My. Since the distribution density in this case is simply the time derivative of the integral distribution it must also obey the power law with an exponent lesser by unity. This is clearly seen from the results of calculations.

The obtained power law character of the interval lengths distribution provides evidence of the scale invariance of durations of constant polarity epochs and the exponent in Eq.(1) presents a quantitative measure of this self-similarity - fractal dimension of the lengths distribution D - that in this case equals 2.0. As to the differential curve, if we regard it as a function of the probability density of values of interval lengths, $p(t) \sim t^{-3}$, we may write a scaling relation

$$p(at) \propto a^{-3} p(t), \qquad (2)$$

valid in the whole scale range where the distribution is proved to be self-similar, i.e. for the intervals longer than 0.3 My. The scaling relation (Eq.2) means that, say, the probability of occurrence of an interval 2 My long is 8 times greater than that for the 4 My interval, but 8 times less than for an interval of 1 My duration. It is important that the scaling relation (Eq.2) fully defines the whole interval distribution - one value of $p(t)$ is enough to restore the whole curve - and represents a quantitative estimation of relative significance of intervals of different duration.

3.2 Box-counting method

The fractal dimension as determined says nothing about the structure of moments of reversals scattered along the time axis. This kind of information may be obtained with the use of the box-covering technique (Forrest and Witten, 1979; Sagdeyev et al., 1988). In this case the results may be interpreted in terms of probabilities of filling of time intervals of different length (Turcotte, 1989).

According to this approach we divide the total time interval T (160 My) into m equal intervals with length of dt (so $T = m \cdot dt$), and estimate the relative number $N_s = Pr(dt)$ of intervals containing at least one event (GMF reversal). Being relative, this number may be regarded as the probability of filling of an interval of a certain length, so it must obviously depend on the length value dt, that is on the scale, and for a scale-invariant set of points one must find that

$$\log(\mathrm{Pr}) \propto C_F \log(dt) \qquad (3)$$

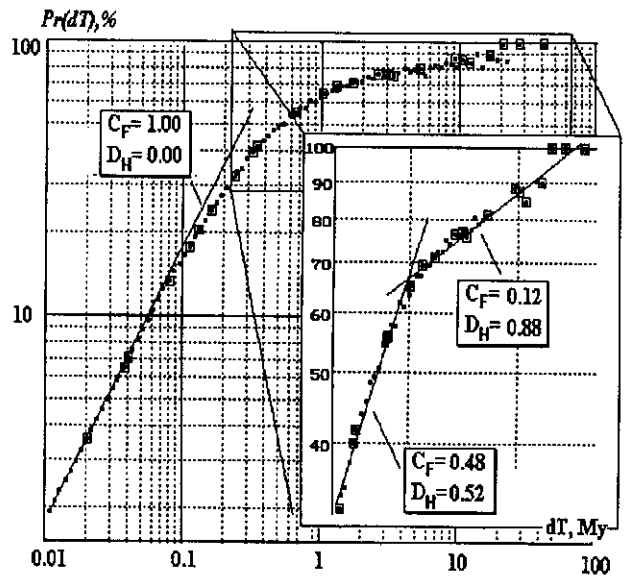

Fig. 3. Dependence of probability of filling of an interval on its duration (box-counting technique). Explanations in text. Inset shows a portion of the graph with exagerrated vertical scale.

so that the dependence is linear on a double logarithmic scale. The fractal (Hausdorff) dimension of the set is

$$D_H = E - C_F,$$

where E is the Euclidean dimension of the embedding space (in our case $E = 1$), and C_F is the scaling exponent from (Eq.3). It is easily seen that the quantity C_F in this case presents the fractal codimension of the set (Schertzer, Lovejoy, 1993).

Application of the box-counting technique to the palaeomagnetic scale enabled us to distinguish the time scale range from 0.2 to 30 My (that is over two orders of magnitude) within which the existence of statistically self-similar properties of the reversal sequence is manifested sufficiently clearly. In Fig. 3 a graph is presented showing the dependence of probability of interval filling on interval duration. Different symbols indicate values obtained by different methods: squares - by consequent dividing of total interval into integer number of equal parts, dots - by consequent double increasing of elementary time interval (10 Ky). It is clear that the former technique must provide more valid probability values for large time intervals, and the latter for the small intervals.

The graph shows that for very small intervals (less than 0.1 My) the corresponding probability grows proportionally with interval length and that for great intervals (longer than 30 My) it is equal to 1. These asymptotic branches of the graph are due to the limited temporal resolution of the data on the one hand, and to the finite total range on the other. Since the total number of events is limited, while decreasing the interval length we inevitably reach the value when no one interval contains more than one event. It occurs when the interval

length becomes less than the predominating minimum duration of uniform polarity (say 0.1 My), and this value depends mostly on scale resolution. In this scale range, the number of filled intervals becomes strictly equal to the total number of registered events N, and

$$Pr(dt) = N/m = (N/T)dt,$$

so that

$$Log\ (Pr) \sim Log\ (dt),\ C_F = 1,$$

and we approach the trivial case of zero dimension of a finite point set ($D_H = 0$). This situation is represented by the left branch of the graph of Fig. 3.

The rightmost branch of the same graph reflects another asymptotic case - gradual saturation of the intervals as the box size grows. When the interval length exceeds the maximum recorded duration of uniform polarity of GMF (that is about 35 My) the share of filled intervals becomes equal to 1 and the graph coincides with horizontal asymptote $Pr(dt) = 1$. In this case one can see that $C_F = 0$ and $D_H = 1$. This means that if temporal resolution relative to the total record length is too poor the time axis is filled entirely.

We are interested first of all in the behaviour of the probability curve in the intermediate scale range (from 0.1 to 30 My) where transition from one asymptote to another takes place. We found that there are two regions of the graph where the curve may be readily approximated with a straight line of the form Eq.(3). The inset in Fig.3 presents this part of the graph with magnified vertical scale. It is easily seen that in the scale range from about 0.2 to 1 My the dependence is linear with the slope of $C_F = 0.48$, which implies fractal dimension of approximately $D_H = 0.52 \pm 0.02$, close to that of Brownian noise. In the temporal scale range from 1 to 30 My the slope of the approximating straight line is $C_F = 0.12$ that proves the statistically self-similar character of events distribution in this scale range with fractal dimension of $D_H = 0.88 \pm 0.02$.

3.3 Dispersion scaling

Additional arguments in favour of the self-similarity of the GMF reversal sequence may be obtained by means of the analysis of the scaling properties of dispersion. Let us define the density of events ρ as the ratio of the number of events n within a certain interval to its length dt ($\rho = n/dt$). If the total time range T is divided into m parts ($T = m\ dt$) then in general individual values of ρ are different. The set of ρ values may be characterized with its mean value ρ_m and mean square deviation σ_m (square root from dispersion) relative to this average. It is evident for any dt that the mean density must be equal to the average density of the whole set, that is $\rho_a = N/T \sim 2$ (My)$^{-1}$. But the density dispersion, generally speaking, will depend on dt value and must decrease with its growth.

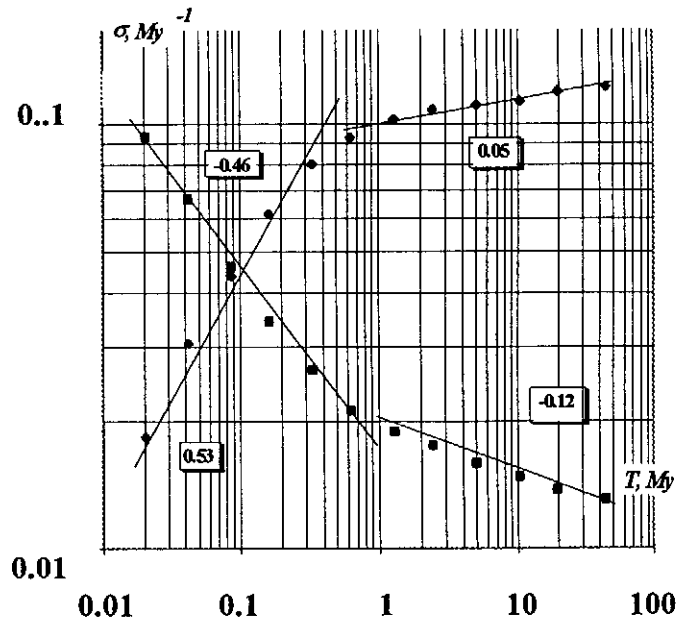

Fig. 4. Results of dispersion counter-scaling technique calculations showing time span dependence of external (squares) and internal (circles) mean square deviation.

If we assume the hypothesis of statistical independence of events and of randomness of their appearance (Poisson process), then we may compare the deviations of density of events along the time axis with density fluctuations of an ideal gas and apply corresponding methods of statistical physics (see, for instance, Reif, 1968) in order to theoretically estimate them. It may be shown that the average number of events within an interval of length dt is $n = \rho_a\ dt$, and the mean square deviation of this number from average is $\sigma_n = (\rho_a\ dt)^{1/2}$. So for mean square deviation of density we obtain

$$\sigma = \sigma_n/dt = \rho_a^{1/2} dt^{-1/2} \approx 1.4 dt^{-1/2}, \qquad (4)$$

which means that for a sequence of independent events the mean square deviation of density is inversely proportional to the square root of the interval length (stochastic case).

If the dispersion scales with time interval with self-similarity exponent $2d$, that is $\sigma = (\rho_a\ dt)^{\ d}$, then the mean square density deviation may be defined as

$$\sigma_n = \rho_a^d dt^{d-1}. \qquad (5)$$

This case is a more general one and includes the Poisson sequence of events with scaling exponent $d = 0.5$

Let us assess now the results of computations of density dispersion of the GMF reversals. The descending plot (circles) on Fig. 4 shows the dependence of mean square density deviation on interval length. An abrupt change can be easily observed by subdividing the whole graph into two different scale ranges. For the intervals less than 0.5 My the dependence is very close to (4), and for intervals greater than 0.5 My it is also rectilinear on

bilogarithmic scale of the type (5) with the slope b=-0.12. The scaling exponent determined from this slope according to (5) characterizes the fractal dimension of the set under study $d = 1+b = 0.88$, that is equal to the value obtained with the box-counting method.

The validity of such an estimate is also demonstrated by the results of application of "dispersion counter-scaling" technique (Ivanov, 1994). This approach regards the above described dispersion as an "internal" one, characterizing statistics of the internal contents of an interval of a certain length. One may also compare the average values of density of different intervals of equal length and obtain an estimate of the "external" dispersion of the set. This quantity must monotonically increase with growth of the time interval, and in the statistically self-similar case scales as dt^{1-d}. The analysis shows (Fig. 4) that in the range of shorter intervals, fractal dimensions defined by scaling exponents of both dispersions are almost equal with regard to calculation errors, giving the average value of 0.505 ± 0.03, close to the dimension of a cut (zeroset) of Brownian noise graph. For intervals more than 0.5 My the situation is essentially different. Although the power law approximation in this case is also good, the scaling exponent of external dispersion in this time span suggests a fractal dimension of the set to be 0.95 ± 0.01 (we remind that internal dispersion scaling gave the value of 0.88). This difference of dimensions obtained from internal and external dispersion scaling, suggests a multi-fractality of the data set; this idea will be tested in the next section.

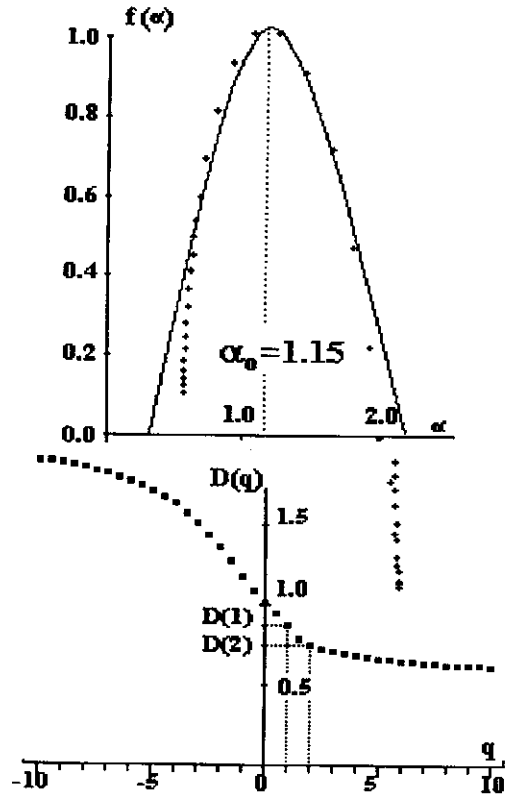

Fig. 5. Multifractal spectra of normalized probabilities of polarity intervals durations. Solid line on the upper graph represents theoretical singularity spectrum of binomial multiplicative process with $p = 0.225$.

3.4 Multifractal properties

As was stated earlier, the difference of values of fractal dimensions obtained by different methods may be due to multiple fractal scaling of the data set. So these results must be appended with multifractal analysis. In our computations we followed mostly the formalism described by J.Feder (1988), though the computational algorithm was original.

The initial sequence of reversals cannot be subjected to multifractal analysis since this involves the assessment of a probabilistic measure. In order to obtain such a measure M we formed a sequence of relative durations of constant polarity intervals $m_i = (T_i - T_{i-1})/T_O$, where T_O is total record length. So the supporting set in this case is simply a segment $[0,N]$, with dimension $E \rightarrow 1$ while $N \rightarrow \infty$, and m_i is a fraction of total time T_O falling into the interval T_O/N. We examined the asymptotic scaling behavior of the quantity τ defined as

$$\tau = log(\Sigma m_i^q)/log(dT),$$

where dT is temporal scale, with $dT \rightarrow 1/N$ for different values of distribution moment q from -10 to 10 with step 0.5. Resulting scaling exponents $\tau(q)$ were further recalculated into multifractal dimension spectrum $D(q)$ and its Legendre transform, the singularity function $f(\alpha)$.

The results of multifractal analysis are presented in Fig.5. The lower panel shows the spectrum of fractal dimensions D with regard to q values. One can see gradual decay of dimension values with increasing moment from 1.91 at q = -10 to 0.61 at q = 10 . There are three points of special interest on the graph. The value $D(0)$, which must represent the geometrical dimension of the supporting set is obtained to be 1.010, which may be regarded as equal to its theoretical value (i.e. unity). The value of information dimension $D(1)$, obtained from the first order moment of the distribution, characterizes scaling of the informational entropy of the measure, and in multifractal context is equal to 0.874 (compare with our previous estimates). Lastly the dimension obtained from the second order moments scaling $D(2)$ = 0.755. Theoretically it must represent the correlation dimension of the set D_C, but is essentially lower than the directly calculated value (0.875 - see next section). We suppose that this difference may be due to the fact that in these two cases we analyzed different sets - the sequence of interval durations in multifractal analysis and the sequence of moments of reversals in correlation integral computations.

The upper panel of Fig.5 presents the $f(\alpha)$ functions, sometimes regarded as a spectrum of singularities of the analyzed set. Its shape is rather symmetric, though there exists a region of negative $f(\alpha)$ values for $\alpha > 2.0$, corresponding to greatest negative values of q. The reasons for such a situation and its meaning were assessed by B.Mandelbrot (1989, p.35), who has shown theoretically that under certain conditions multifractals, generated by multiplicative processes, may be characterized by negative values of $f(\alpha)$ for some α values. He called them "latent α's" in contrast to "manifest α's", for which $f(\alpha)$ is positive and even described a situation when $f(\alpha_{max}) = -\infty$. In our case, as it is seen in the plot, all α's for $\alpha > 2$ are "latent".

The symmetric form of the curve resembles that characteristic of a binary multiplicative process, that is generally regarded as a typical multifractal generating process. It consists of the redistribution of initially uniform probability on a segment into two halves in proportion p and $1-p$. Theoretical assessments show the existence of a relation between p and the value of α_0 where $f(\alpha)$ reaches its maximum in the form

$$\alpha_0 = -\frac{\ln p + \ln(1-p)}{2\ln 2}.$$

Therefore one may determine the p value using $f(\alpha)$ curve. The p value, obtained from the experimental curve of Fig.5 is equal to 0.225.

3.5 Correlation dimension analysis

The above presented results clearly show power-law dependencies of different statistical characteristics of the geomagnetic reversal sequence, and suggest that the process resulting in GMF reversals is deterministic rather than stochastic. In order to test this suggestion we examined the reversal sequence as an output of a dynamic system, trying to trace its trajectory in the phase space following the widely applied correlation method (Grassberger and Procaccia, 1983; Grassberger, 1986).

Regarding each moment of reversal T_i as a state parameter we studied the behavior of correlation integral

$$N(t) = N_{i,j}\{dt_{i,j} > t\},$$

or in other words, number of pairs of points $N_{i,j}$ in phase space with distance between them exceeding t. If the correlation integral scales with t according to power law, its scaling exponent represents the correlation dimension D_C. The procedure includes calculations of $N(t)$ in phase space of different integer dimensionality E, where phase coordinates are *[Ti , Ti-1 , Ti-2...Ti-E]*. We made our estimates for all E from 1 to 10. The correspondence of the maximum embedding dimension and the correlation dimension is discussed in the next section.

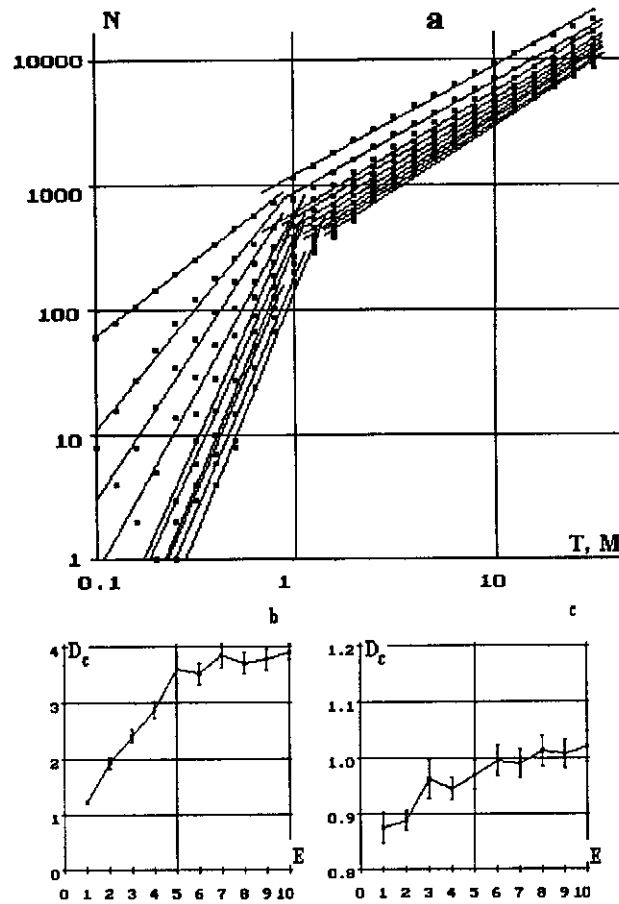

Fig. 6. Results of dimensional analysis of reversal sequence. Graphs of correlation integral vs time span for consequent integer embedding dimensions from 1 (top) to 10 (bottom) with best fit linear approximations (a), and dependence of correlation dimension on dimension of embedding phase space for time spans less (b) and greater (c) than 1 My. Vertical lines - error bars.

Figure 6 presents the results of correlation dimension analysis. The upper panel shows the dependence of correlation integral on time interval for embedding phase space dimensions from 1 (upper graph) to 10 (lower graph). It is clearly seen that each graph contains a crossover point that subdivides it into two parts with different scaling exponents. The average position of this point is about 1 My; the slope for greater time intervals is approximately the same and close to 1, while for lesser intervals gradual steepening of the log-log plot with increasing embedding dimension is observed.

The lower panel of Fig.6 and Table 1 illustrate changes of scaling exponents of correlation integral (that is correlation dimension Dc) with phase space dimension. For time intervals less than 1 My (Fig.6b) Dc almost linearly increases up to $E = 5$ where it reaches a kind of asymptotic regime. The average value of the correlation dimension for E from 5 to 10 is. estimated to be 3.72 ± 0.20. Time intervals from 1 to 30 My are characterized by a more uniform correlation dimension (Fig.6c - note that vertical scale is magnified relative to that of the previous

Table 1. Values of correlation dimension of palaeomagnetic reversal sequence for different integer dimensions of embedding phase space in two major temporal ranges

Dimension of embedding phase space	Correlation dimension	
	0.1 - 1.0 My	1.0 - 30 My
1	1.213 ± 0.018	0.875 ± 0.027
2	1.928 ± 0.091	0.888 ± 0.017
3	2.407 ± 0.114	0.964 ± 0.036
4	2.874 ± 0.144	0.944 ± 0.021
5	3.589 ± 0.244	0.971 ± 0.025
6	3.516 ± 0.182	0.995 ± .027
7	3.845 ± 0.216	0.990 ±0.024
8	0.990 ±0.024	1.011 ±0.026
9	3.763 ± 0.193	1.007 ± 0.026
10	3.907 ± 0.140	1.020 ± 0.027

graph). Here we may observe more definite asymptotic behavior of Dc for embedding dimensions greater than 5, and individual values of Dc are approximately 1.0 within the calculation error (mean value is 1.00 ± 0.02). For embedding dimensions >2 deviations of Dc from asymptotic value do not exceed 10%.

So these calculations suggest a low dimensionality of attractor of the possible underlying dynamic system, and the dimension value is different in different temporal regions.

4 Discussion

Generally speaking the idea of scale invariance of the GMF reversal sequence was implicitly suggested by the author of the palaeomagnetic scale (Cox., 1982) in the very terminology of the epochs of different behavior of the GMF. He introduced the notions of subchrons, chrons, superchrons and hyperchrons of geomagnetic polarity, the length of which consequently increases by a decimal order of magnitude - about 0.1, 1, 10 and 100 My respectively. (It must be noted here that the palaeomagnetic scale though with lower resolution is traced down to 450-500 Ma, and this gave the grounds to enter such a unit as hyperchrone.)

The reported results provide an opportunity to put these intuitive assumptions on a quantitative base. Table 2 summarizes the values of fractal dimension of analyzed reversal durations obtained in this study by different methods. The most striking feature of these results is the existence of a crossover point that divides total temporal interval into two different parts with different scaling

Table 2. Summary of fractal dimension values of palaeomagnetic reversal sequence obtained with different methods for different temporal intervals and the position of the crossover point.

	Crossover point position	Fractal dimension	
	(dt_{cr}, My)	$dt < dt_{cr}$	$dt > dt_{cr}$
Intervals distribution	–	1.98	
Box-counting technique	1.0	0.52	0.88
Dispersion scaling analysis			
internal	0.5	0.54	0.88
external	0.5	0.47	0.95
Correlation integral scaling	1.0	1.21	0.88
Multifractal analysis			
information dimension	–	0.87	
correlation dimension	–	0.76	

properties. The position of this crossover point varies from 0.5 to 1.0 My for different methods. This temporal subdivision is not only manifested in the interval distribution, where in our opinion the bulk characteristics of distribution predominate, but also in the results of the multifractal analysis, which formally implies the existence of uniform scaling.

Though the time spans covered by these dependencies are not large (each about 1.5 decimal orders of magnitude) the fitness of calculated quantities to straight lines in log-log scale in all cases is good enough to assure the power law character of the dependencies and the statistical self-similarity of the data set. Since we are dealing with an output of a certain physical process and are inevitably limited by the data resolution on one side and by sample volume on another, we may only consider its intermediate asymptotics (Barenblatt, 1978), and so can regard our results as a reliable analysis of real data.

Another essential result of this study is the value 0.88, obtained for the fractal dimension of reversal sequence for time intervals greater than 0.5-1.0 My. It is derived by four different methods and therefore may be accepted as a representative value of the (mono)fractal dimension for longer time intervals, and as such may be used as a quantitative statistical measure for testing various models of GMF reversals. As to the interval durations below the crossover point, the box-counting and dispersion scaling techniques give the fractal dimension of the set close to 1/2, which may indicate stochasticity of data (a Poisson--like sequence of independent events). But other methods suggest other values of fractal dimension, evidencing

some clustering of points in this time span, and the question of whether the underlying process is random or deterministic in this interval cannot be definitely answered on the base of these computations.

It was natural to suppose *a priori* that such a complex system as the Earth's magnetic generator may generate a multifractal output. The results of multifractal analysis clearly confirm this suggestion. They also add some new topics for discussion, by which we mean the symmetry of the singularity spectrum and, the above mentioned possibility that the interval durations may be simulated by a binary multiplicative process. The bulk average value of binary measure p was presented in Section 3-4 and was estimated to be about 0.225. We tried to test this estimate directly, computing the relation between probabilities of two adjacent intervals in the process of successive division of the total segment into 2^n parts. Figure 7 shows the resulting graph, representing the dependence of measure p on temporal interval. A tendency of increasing p values for lesser time intervals is observed. For intervals less than 0.2 My these values reach the theoretical value of 0.5, that means that for lesser intervals the probability is divided into equal parts between two halves of the interval. This probably indicates that the multifractal (and fractal) properties of the set gradually decrease at these scales. It is not yet clear whether this may be an artefact caused by lack of resolution of the data. For longer time intervals, on the contrary, resolution is sufficient, but the number of data is too poor to obtain reliable statistics and the error bars reflect this situation.

In any case in the greater part of the temporal domain we observe scaled power-law behaviour of binary coefficient. It seems that here we encounter a special and more general case of a multifractal - a multiscaled multifractal. Thus, a classical binomial multiplicative process has a constant value of p in the whole scale range. If p scales with resolution it means that multifractality changes with scale, and results obtained with routine methods are not as reliable as they seem to be. But this is a special problem that lies beyond our assessment here.

The clustering of reversals in time may be a manifestation of the self-organization of the non-linear magneto-hydrodynamic processes within the liquid Earth's core, responsible for the GMF reversals. If so, the corresponding dynamical system must be characterized by an attractor of low dimension, say less than 10. Up to date a number of low-dimensional models of dynamical systems with chaotic output have been suggested, among them several directly referring to the Earth's dynamo (Rikitake, 1958; Lorenz, 1963; Robbins, 1976; Chillingworth and Holmes, 1980). The output of such models, though chaotic, is not random since it is governed by deterministic dynamics. Both model and real reversal sequences have been thoroughly analyzed in this context (Chillingworth and Holmes, 1980, Dubois and Pambrun,

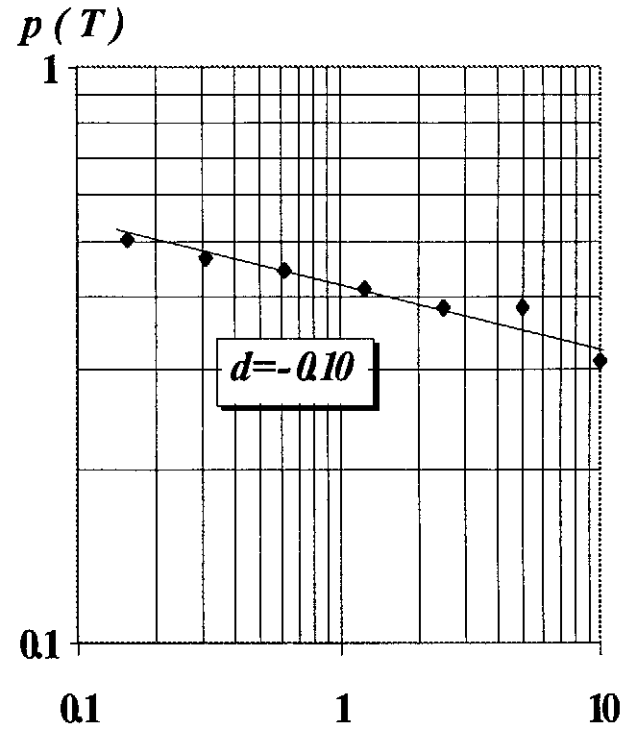

Fig. 7. Scaling of binary coefficient p. Explanations in text.

1990, Cortini and Barton, 1994 and others). The common point of view on this problem is that although the dimension of the attractor of all of these models is very low (mostly close to 1), the dimension of the attractor of the actual set of reversals appears to be essentially greater, and the authors give only the lower limit of correlation dimension of the GMF reversals dynamics - e.g. an estimate of $D_C>3$ in Cortini and Barton (1994)

Our study adds some new details to this subject. Dimensional analysis presented in Section 3.5 shows that the attractor of experimental reversal sequence is not statistically uniform over the total time scale range. Here we also find a crossover point at approximately 1.0 My, subdividing scale subranges with different scaling behaviour of correlation integral, as it was in the case of direct fractal (and multifractal) analysis. In some sense one may say that here we deal with two different attractors, one of which describes long-term processes and the other short-term ones. It seems that convergence of the correlation dimension of the long-term attractor to a value close to 1 is close to the ideal (Fig.6c), while in the case of the short term attractor (Fig.6b) there remains some doubt. Nevertheless, in our opinion convergence of its dimension to the value of $D_C = 3.7$ is also rather good. This conclusion is supported by the existence of a sharp change of the form of the graph $D_C(E)$, that occurs at $E = 5$. We also take into account the consideration of F.Takens (1981), who suggested that convergence of correlation dimension is reliable if $D_C(E)$ is traced up to

$E \geq 2D_C+1$ (Ord, 1994) This condition is satisfied in our analysis. So we may state that the geomagnetic dynamical system as a whole may be presented as a superposition of a very low-dimensional system, that may be described by a disk dynamo model with $D_C \approx 1$, and a relatively high-dimensional (or, that is less probable, stochastic) system ($D_C \approx 3.7$ or greater). Each of these systems occupies different and non-overlapping temporal domains.

.In this context it might be very useful to assess coupling of the Earth's magnetic dynamo with other terrestrial and extraterrestrial systems, able to influence the GMF dynamics. This problem was outlined by Cortini and Barton (1994), and we think that our results may provide new insight to this discussion. The existence of two different temporal domains of GMF dynamics may arise from a great gap in viscosity between inner geospheres (core, mantle and lithosphere, that is solid Earth) and outer medias (hydro- and atmosphere and space). The interactions of internal and external field-generating systems may be non-linear and different at different time scales. From this point of view, attempts at estimating the dimensionality of the Earth's climatic system (Nicolis and Nicolis, 1984, Grassberger, 1986 and others), which itself is a product of interaction of a number of different driving agents, are interesting, since they also deal with a result of non-linear coupling of various internal and external factors.

The search for hidden signs of self-organization in various geophysical processes on the basis of the analysis of self-similarity of their manifestations is only getting started. From our point of view it would be very interesting to analyze in a similar way other global processes in the geological history of the Earth, at least those whose intensity in time may be quantitatively estimated, such as tectonic activity, and so on. Comparison of these results may provide knowledge of interrelations of different phenomena in the Earth's history and other key problems of global evolution.

Acknowlegements. The author is grateful to Prof. A.S.Monin and Prof. G.I.Barenblatt for helpful discussions and to anonymous reviewers, whose scrupulous comments and remarks were very useful for preparation of the final version of the paper. Some previous results were reported at the conference "Nonlinear variability in geophysics" (Cargese, France, 1993) and the author is very grateful to Prof. D.S.Schertzer and Prof. D.L.Turcotte for their critical and positive comments on the subject. The study was partly supported by the Russian Basic Researches Foundation (grant RBRF # 93-05-8943).

References

Barenblatt, G.I. *Self-similarity, Intermediate Asymptotics.* (Russian edition : Moscow, Gidrometeoizdat, 1978)

Chillingworth, D.R.J. and Holmes, P.J. Dynamical systems and models for reversals of the Earth's magnetic field. *Mathematical Geology, v.12,* No. 1, 41-59, 1980

Cortini, M and Barton., Ch. Chaos in geomagnetic reversal records: A comparison between Earth's magnetic field data and model disk dynamo data. *J. Geoph. Res., vol.99,* No. B9, 18021-18034, 1994

Cox, A.V. Magnetostratigraphic time scale. In: Harland, W.B. et al, eds, *A Geologic Time Scale.* Cambridge Univ. Press, Cambridge, 63-84, 1982

Dubois, J. and Pambrun, C. Etude de la distribution des inversions du champ magnetique terrestre entre - 160 Ma et l'actuel (echelle de Cox). Recherche d'un attracteur dans le systeme dynamique qui les genere. *C.R. Acad. Sci. Paris, t.311,* Serie II, 643-650, 1990

Feder, J. *Fractals.* Plenum Press, New York, 1988

Forrest, S.R. and Witten, T.A., Jr. Long-range correlation in smoke particle aggregates. *J. Phys., A, 12,* L109-117, 1979

Fraedrich, K. Estimating the dimensions of weather and climate attractors. *J. Atm. Sci., 43,* No. 5, 419-432, 1986

Grassberger, P. Does climatic attractor exist? *Nature, 323,* 609-612, 1986

Grassberger, P. and Procaccia, I. Measuring the strangeness of strange attractors. *Physica D, 9,* 189-208, 1983

Hilgen, F.J. Astronomical calibration of Gauss to Matuyama sapropels in Mediterranean and implication for the Geomagnetic Polarity Time Scale. *Earth and Plan. Sci. Letters, v. 104,* 226-244, 1991a.

Hilgen, F.J. Extension of the astronomically calibrated (polarity) time scale to the Miocene/Pleistocene boundary. *Earth and Plan. Sci. Letters, v. 107,* 349-368, 1991b.

Ivanov, S.S. "Counter-scaling" method for estimation of self-similarity of self-affine objects. In: J.H.Kruhl, ed., *Fractals and Dynamic Systems in Geosciences,* Springer, Berlin Heidelberg New York, 391-397, 1994.

Korvin, G. *Fractal Models in Earth Sciences.* Elsevier Publ., Amsterdam, 1992

Lorenz, F.N. Deterministic nonperiodic flow. *J. Atmospheric Sci., v. 20,* 130-141, 1963

Lowrie, W. Geomagnetic reversal history. *Terra Nova, 2,* 438-445, 1991

Mandelbrot, BB. *The Fractal Geometry of Nature.* Freeman, New York, 1983

Mandelbrot, B.B. Multifractal measures, especially for the geophysicist. *PAGEOPH, vol. 131,* N0. 1-2, 5-42, 1989

Mazaud, A., Laj, C., de Seze, L., and Verozub, K.L. 15-Myr periodicity in the frequency of geomagnetic reversal record. *Nature, 334,* 328-330, 1983

Naidu, P.S. Statistical structure of geomagnetic field reversals. *J. Geophys. Res. 76,* 2649-2662, 1970

Nicolis, C. and Nicolis G. Is there a climatic attractor? *Nature, 311,* 529-532, 1984

Ord, A. The fractal geometry of patterned structures in numerical models of rock deformation. In: J.H.Kruhl, ed., *Fractals and Dynamic Systems in Geosciences*, Springer, Berlin Heidelberg New York, 131-155, 1994.

Prevot, M., Mankinen, E.A., Gromme, C.S., and Coe, R.S. How the geomagnetic field vector reverses polarity. *Nature, 316*, 230-234, 1985

Reif, F. Statistical Physics. McGraw-Hill Book Co., 1968

Rikitake, T. Oscillations of a system of disk dynamos. *Proc. Cambr. Phil. Soc., v. 54*, 89, 1958

Robbins, K.A. A moment equation description of magnetic reversals in the Earth. *Proc. Natl. Acad. Sci. U.S.A., v.73*, 4297-4301, 1976

Sagdeyev, R.Z., Usikov, D.A. and Zaslavsky, G.M. *Nonlinear Physics - From the Pendulum to Turbulence and Chaos*. Charwood, Chur, Switzerland, 1988

Schertzer, D., Lovejoy, S. *Scaling and multifractal processes*. Lecture Notes, Cargese, 1993, 292 p.

Shackleton, N., Berger, A. and Peltier W.R. An alternative astronomic calibration of the Lower Pleistocene time scale based on ODP site 677. *Trans. Roy. Soc. Edinb.: Earth Sci., v. 81*, 251-261, 1990

Takens, F. Detecting strange attractors in turbulence. In: Rand, D.A.and Young, L.S. eds. *Dynamical Systems and Turbulence.Lecture Notes in Mathematics. 898*, Springer, New York, 366-381, 1981

Tritton, D.J, Deterministic chaos, geomagnetic reversals, and the spherical pendulum. In: Lowers, F.J. et al, eds. *Geomagnetism and Paleomagnetism*. Kluwer Acad. Publ., 215-226, 1989

Turcotte, D.L. Fractals in Geology and Geophysics. *Pure Appl. Geoph., 131*, N 1/2, 171-195, 1989

Turcotte, D.L. Crustal deformation and fractals: a review. In: *J.H.Kruhl, ed., Fractals and Dynamic Systems in Geosciences*, Springer, Berlin Heidelberg New York, 7-23, 1994.